CHAPTER 6

Applications of Polarized Electron Sources Utilizing Optical Orientation in Solids*

D.T. PIERCE and R.J. CELOTTA

National Bureau of Standards, Washington, D.C. 20234 U.S.A.

*Supported in part by Office of Naval Research.

Optical Orientation
Edited by
F. Meier and B.P. Zakharchenya

Contents

1. Introduction

The optical orientation of electron spin in semiconductors provides the basis for the most intense and well controlled source of spin polarized free electrons that exists today. As such, optical orientation fulfills a need dating back to the discovery of electron spin by Goudsmit and Uhlenbeck (1925). One might expect that it would be possible to obtain a polarized electron beam by passing electrons through an inhomogeneous magnetic field in a Stern–Gerlach type experiment. However, an uncertainty principle argument attributed to Bohr (Mott 1929) shows that, in contrast to a beam of neutral atoms in a conventional Stern–Gerlach experiment, the spreading of the (charged) electron beam in the magnetic field is such as to mask any separation of electrons of different spin orientation. Mott (1929) showed theoretically that it should be possible to obtain a beam of polarized electrons (or spin analyze an already polarized beam) in electron scattering from the Coulomb field of a heavy nucleus. Several attempts were made to observe electron spin polarization in the scattering experiment suggested by Mott, but it was not until 1943 that spin polarization in a free electron beam was first observed (Shull et al. 1943). In 1956, Lee and Yang predicted the nonconservation of parity in weak interactions and its manifestation as a spin polarization of electrons emitted in β decay. However, neither Mott scattering nor β decay is generally suitable as a source of polarized electrons for other experiments. In the last twenty years, a variety of spin dependent processes have been discovered and used to provide beams of polarized electrons. Some of the more promising of these – chemiionization of optically oriented metastable helium, photoionization of polarized atoms, the Fano effect, field emission from a ferromagnet, and photoemission from optically oriented GaAs – have been compared in a recent review (Celotta and Pierce 1980).

Optical orientation of electrons in GaAs with a surface treated to obtain negative electron affinity (NEA), and hence efficient electron emission, was proposed for a source of polarized electrons by Garwin et al. (1974) and Lampel and Weisbuch (1975). The fact that optically oriented electrons can be photoemitted from NEA GaAs and do indeed maintain a high spin polarization was reported by Pierce et al. (1975a, b). Based on this work, a number of electron sources have been designed and applied to a wide range of experiments. In sect. 2 we describe the principles of the GaAs polarized electron

source such as the transport and emission of the optically oriented electrons and the possibility of depolarization. The general requirements which must be met by a polarized electron source and the corresponding characteristics of the GaAs source are discussed. Different specific experimental requirements and different approaches to source construction have resulted in some variety in existing GaAs sources which will be briefly discussed with references given to more complete descriptions. Ways in which a beam with higher spin polarization might be obtained are discussed.

The applications of a spin polarized electron beam from optically oriented GaAs range over diverse fields – atomic and molecular physics, condensed matter physics, nuclear physics, and elementary particle physics. The spin dependent effects arise from the spin–orbit interaction, the exchange interaction, and the parity violating effects of the weak interaction. For this chapter, we have selected examples from three fields to give some flavor of the diversity and fruitfulness of this application of optical pumping in solids.

In sect. 3 we describe a "perfect" scattering experiment (Wübker et al. 1982) in which polarized electrons were scattered from Xe to obtain a complete description of the scattering in terms of the direct and the spin-flip scattering amplitude and the phase between them. The spin–orbit interaction is the source of the spin dependence in this experiment.

In sect. 4 the scattering of a spin polarized electron beam from the surface of a ferromagnet is seen to be a sensitive probe of surface magnetism. The spin dependence of the scattering is due to the exchange interaction between the polarized incident spin and the oriented spins of a ferromagnetic surface. Polarized electron scattering allows the measurement of hysteresis curves of the outer few layers of a magnetic surface (Unguris et al. 1984). At low temperatures, differences between the temperature dependence of the surface and bulk magnetizations have been measured (Pierce et al. 1982). The critical exponent of the surface magnetization has been determined by temperature dependent, polarized, elastic electron scattering studies near the Curie temperature (Alvarado et al. 1982a, b). A type of inelastic scattering of a polarized electron beam in which a photon is emitted, known as spin polarized inverse photoemission, is shown to provide a new spectroscopy of the unfilled states of a ferromagnetic solid (Unguris et al. 1982).

In sect. 5, the application of a polarized electron beam to study parity violation in deep inelastic scattering of polarized electrons and polarized hydrogen (Prescott et al. 1978, 1979) is described. These landmark experiments represent an important experimental test of the unified theory of weak and electromagnetic interactions for which Weinberg and Salam recently received the Nobel Prize.

Many other examples of applications of a spin polarized electron beam from optically oriented GaAs could be discussed as well as a number of applications in progress or proposed. In nuclear physics for example, an experiment is

under way (McDonald 1980) to study the weak nucleon–nucleon interaction by using an intense beam of polarized electrons to generate circularly polarized bremsstrahlung and measure the asymmetry in the photodisintegration of deuterium ($d+\gamma \rightarrow n+p$). Feinberg (1975) has discussed asymmetries in the polarized electron–nucleus scattering due to parity violating, neutral current interactions. There are several review articles which may be useful to readers interested in further applications of polarized electron beams: on scattering from atoms (Kessler 1976, Lubell 1980, Celotta and Pierce 1982), on scattering from surfaces (Pierce and Celotta 1981, Feder 1981), on spin polarization in solid state physics in general (Siegmann et al. 1984), and on applications of polarized electrons in high energy physics (Prescott 1981, Hughes 1981).

2. *Spin polarized electron source using optically oriented GaAs*

2.1. *Production of polarized electron beams*

The photoemission of spin polarized electrons from negative electron affinity (NEA) GaAs surfaces has been discussed (Pierce and Meier 1976) in terms of the three step model (Spicer 1958) of the photoemission process: photoexcitation, transport to the surface, and escape into vacuum. The polarization P of the photoemitted electrons depends on the initial polarization P_i of the electrons in the conduction band and on any depolarization that takes place before they have escaped into the vacuum. The initial polarization is the result of the optical orientation which occurs in the photoexcitation process and is discussed in depth elsewhere in this book. This is summarized for GaAs in fig. 1 which shows the energy bands near the center of the Brillouin zone. As a result of spin orbit coupling, the 6-fold degenerate p band is split into a 4-fold degenerate $P_{3/2}$ level and a 2-fold degenerate $P_{1/2}$ level, separated by 0.34 eV at the valence band maximum. The corresponding m_j sublevels and relative intensities of the possible transitions with the selection rule $\Delta m_j = \pm 1$ for $\sigma^{\pm}$ circularly polarized light are shown on the right of the figure. The initial polarization is $P_i = \mp 0.5$ for excitation from the valence band maximum to the conduction band minimum with $\sigma^{\pm}$ light. The ease of polarization reversal by simply switching between σ^+ and σ^- light, without changing any other parameter of the resultant electron beam including the intensity, is a feature of the optical orientation process which is very important for the polarized electron source.

Normally, electrons which are excited to the conduction band minimum do not escape from the solid but rather recombine. In fact, the electron affinity which is the difference in energy between the conduction band minimum and the vacuum level, the energy to which an electron must be excited to escape

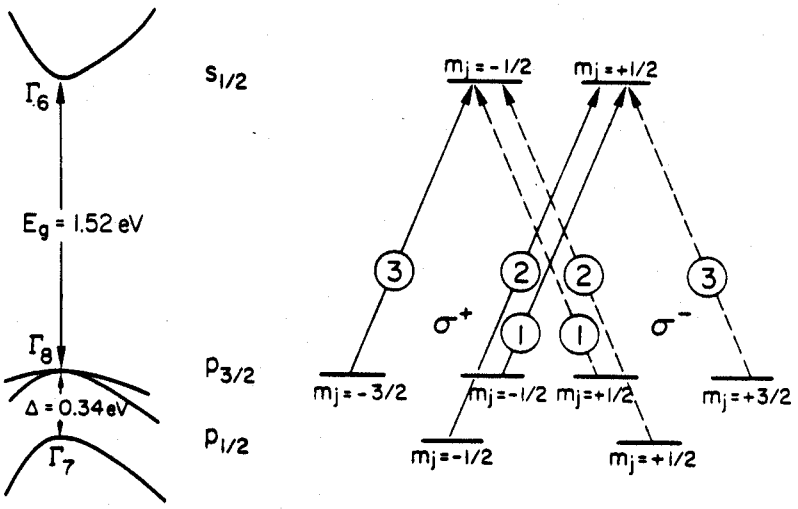

Fig. 1. The energy band diagram, E vs k, of GaAs near the center of the Brillouin zone shows the spin–orbit splitting Δ of the valence bands and the energy gap E_g. On the right, the relative intensities (circled numbers) are given for transitions between m_j sublevels with σ^- and σ^+ circularly polarized light shown by solid and dashed lines respectively. If electrons are excited with circularly polarized light only from the valence band maximum, three times as many of one spin are excited as of the other. (From Pierce and Meier 1976.)

into the vacuum, is approximately 4 eV for a clean GaAs surface. The ability to obtain intense polarized electron beams from GaAs relies on a remarkable property of GaAs and closely related III–V compounds: by appropriate treatment of the surface with cesium and oxygen it is possible to lower the vacuum level at the surface below the level of the conduction band minimum in the bulk, a condition which has been termed "negative electron affinity." Electrons which are excited in an NEA cathode, as shown in fig. 2, thermalize to the conduction band minimum and can diffuse to the surface where no barrier prohibits their emission. The electrons are excited in a region determined by the light absorption length α^{-1} which is on the order of 1 μm. Since the diffusion length is also approximately 1 μm, a very large fraction of the photoexcited electrons are emitted. In fact, NEA GaAs is an extremely efficient photoemitter and is therefore used in photomultiplier tubes and a number of other devices (Bell 1973).

In contrast, in the case of a positive electron affinity electrons excited to energies above the barrier can lose energy by electron–phonon scattering such that they fall below the vacuum level and are no longer emitted. The region from which electrons are emitted is then determined by the electron–phonon scattering length which is on the order of 100 Å. For a large electron affinity,

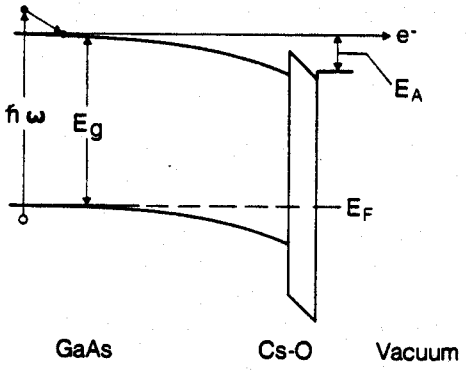

Fig. 2. The energy levels shown as a function of position for the GaAs, Cs–O layer and vacuum. The valence band and conduction band of p-type GaAs bend downwards in energy at the surface. A negative electron affinity E_A (vacuum level lower than the bulk conduction band minimum) is obtained by activation with Cs and O_2. Very high photoyield is obtained because electrons that are excited across the band gap E_g by photons of energy $\hbar\omega$ thermalized to the conduction band minimum, diffuse to the surface, and escape without encountering a barrier. (From Pierce et al. 1980.)

as in the case of a clean GaAs surface, electron–electron scattering dominates and the escape depth of photoelectrons is much smaller, on the order of 10 Å.

The steady state polarization of electrons in the conduction band, P_c, depends on the spin relaxation time τ_s relative to the time τ before an electron recombines as discussed in previous chapters. It is determined from the recombination luminescence polarization $P_r = P_c P_i$. In the case of photoemission, an electron must escape before it recombines so the relevant electron lifetime is shorter, and therefore the polarization P of the photoemitted electrons is higher than P_c. Generalizing the one-dimensional diffusion model of Bell (1973) to include spin polarization, and making approximations appropriate for the case of GaAs, the polarization of photoemitted electrons was found to be (Pierce et al. 1980).

$$P = \frac{\alpha + 1/L}{\alpha + 1/l} P_i, \tag{1}$$

where $L = \sqrt{D\tau}$ is the diffusion length, D is the electron diffusion coefficient, and $l = \sqrt{DT}$ is a spin memory diffusion length, where $1/T = 1/\tau + 1/\tau_s$.

Lampel and Eminyan (1980) showed how this result could be related to the steady state polarization. Using the same generalized one-dimensional diffusion equations they found

$$P_c = P_i \frac{\tau_s}{\tau + \tau_s} \frac{(\alpha L + 1)}{(\alpha l + 1)} \tag{2}$$

so that

$$P = P_c\left(\frac{\tau + \tau_s}{\tau_s}\right)^{1/2}. \tag{3}$$

Thus the polarization of the photoemitted electrons is always greater than the steady state conduction band polarization which one would determine from a luminescence measurement. Lampel and Eminyan (1980) verified this relationship experimentally at a photon energy, $\hbar\omega = 1.55$ eV, just greater than the band gap, by determining P_c from luminescence measurements and P from a measurement of the photoelectron polarization from the same sample.

The sample preparation required to obtain spin polarized photoelectrons is very different from that required to make an optical measurement such as of the luminescence. The GaAs photocathode must be maintained in ultrahigh vacuum, generally in the 10^{-10} Torr range. Before the GaAs surface is treated with cesium and oxygen to obtain a negative electron affinity, it must be atomically clean. This has been achieved for polarized electron sources by first chemically cleaning a GaAs wafer and then heat cleaning in ultrahigh vacuum (Pierce et al. 1980), by cleaving a GaAs single crystal in ultrahigh vacuum (Reihl et al. 1979), and by actually growing a fresh GaAs surface in situ by molecular beam epitaxy (MBE) (Alvarado et al. 1981a). It is interesting to note that the polarization of photoelectrons has been found to approach P_i more closely for thin MBE layers than for bulk crystals (Alvarado et al. 1981a). This can be understood if the photoexcited electrons in the substrate do not readily traverse the interface to the MBE layer. Then, when the thickness of the MBE layer is less than the diffusion length, the photoemission time is shorter and there is less time for spin relaxation.

GaAs spin polarized electron sources built by various groups differ in other ways such as the material chosen and the light source used for optical orientation. "GaAs spin polarized electron source" is used in a generic sense since ternary alloys of GaAs such as $Ga_{1-x}Al_xAs$ (Ciccacci et al. 1982) and $GaAs_{1-x}P_x$ (Conrath et al. 1979) have been used. The aim here has been to tune the band gap to a convenient laser line, e.g. HeNe at 632.8 nm. Polarizations comparable to those obtained from pure GaAs are observed from ternary compounds at compositions up to the direct gap limit (Ciccacci et al. 1982, Reichert and Zähringer 1982). A positive electron affinity surface, while not optimal, was shown to be workable with a HeNe laser (Reihl et al. 1979). Photoelectrons from the NEA GaAs surface can be obtained using the very convenient GaAlAs diode lasers (which now are available with intensities up to 30 mW) or, if more power is required, a Kr ion laser. For the SLAC experiment (Prescott et al. 1978) a pulsed beam of polarized electrons was required and a flash lamp pumped dye laser was used as discussed in sect. 5.

2.2. Characteristics of the source

There are several parameters which specify a source of spin polarized electrons. Some range of variation of the parameters is possible for a GaAs source so that its design can be tailored to the requirements of the specific application. The figure of merit P^2I can be used in characterizing a polarized electron source when counting statistics are the chief source of experimental uncertainty. However, it is not always possible to trade the polarization of the source P against the current it produces I. Because of systematic errors some minimum P is required for a measurement. Furthermore, there may be limitations on the maximum usable current, for example to avoid target damage.

The electron beam current depends on the quantum yield of the photocathode and the intensity of the light incident on it. The quantum yield for the NBS GaAs polarized electron source is typically 20 μA/mW. The maximum d.c. current which has been reported (McDonald 1982) is on the order of 1 mA and was obtained from a GaAs source specially designed for the photodisintegration of deuterium experiment. Beam currents of up to 60 A in a 1.5 to 2 ns pulse, corresponding to a space charge limited current density of 180 A/cm^2, have been reported by Sinclair (1981). Since greater beam current densities can be obtained than with ordinary thermionic emitters and the time structure of the beam is so readily controlled by controlling the light pulse, the GaAs cathode is being used for high current, short pulse applications where spin polarization is not even required (Sinclair and Miller 1981).

The maximum polarization that can be obtained from a negative electron affinity GaAs source has a theoretical limit of 50%. In practice, the polarization obtained is less, owing to the depolarization effects discussed above. For the NBS source, polarizations were measured (Pierce et al. 1980) to be $43 \pm 2\%$ at liquid nitrogen temperature and $36 \pm 2\%$ at room temperature. The theoretical limit for P from an NEA GaAs source has been approached in the case of a thin Be doped GaAs (111) surface produced by molecular beam epitaxy, where $P = 49\%$ was observed (Alvarado et al. 1981a). The reduced depolarization in the thin layer leads to a higher polarization of the electron beam with some sacrifice in the quantum yield.

The possibility of modulating the spin polarization at a desired frequency or with an arbitrary time structure is important for most applications. An electron source utilizing optically oriented GaAs is superb in this regard. The polarization can be reversed without changing the intensity of the beam or any other beam parameter such as the energy, position, or angle. Furthermore, the polarization can be modulated up to the high frequencies attainable with electro-optical modulators. Sine wave or square wave modulation is used in experiments such as those described in sect. 4 in which the changes in an experimental parameter which are in phase with the spin polarization modula-

tion are detected with lock-in techniques. In the high energy experiment described in sect. 5, a random time structure of the polarization reversal was used to minimize possible systematic effects in the small measured asymmetries.

The polarization of the photoemitted electrons is along the incident light axis. Since the electron beam is typically extracted in this direction, its polarization is longitudinal. It is customary to bend the beam by 90° to allow a clear path for the illumination of the cathode. When the electron beam is deflected 90° in a magnetic field the spin is also rotated 90° and the longitudinal polarization is maintained. When the electron beam is electrostatically deflected by 90°, the spin direction is unchanged and the resultant beam is transversely polarized. Both longitudinal and transversely polarized electron beams are used in the applications described below.

The cathode lifetime, or equivalently the stability of the quantum yield, depends on several variables. The current from a cathode under constant illumination typically decreases to 1/e of its initial value in times ranging from several hours to several days. The main mechanism is slow cesium desorption, and cathodes are usually easily restored by adding cesium. This cesium desorption depends not only on the chamber configuration and cesium background but also on the quality of a particular activation. Another source of cathode degradation is due to contaminants which come from electron stimulated desorption from electron optical elements which intercept the electron beam. If the cathode is operated at low temperature, cryopumping of residual gases can also reduce cathode efficiency. In contrast to the intensity, the spin polarization from GaAs photocathodes has been reported as stable even when the quantum yield has decreased by a factor of three from its maximum (Pierce et al. 1980). Changes in polarization of a "few percent" were reported for 3–4 day old cathodes with 1/e intensity decay times of 15–20 hours (Alvarado et al. 1981a).

In order to take advantage of high electron currents from an electron source, its electron optical parameters must be matched to the device or experiment to which it is coupled. Electron optically, a source is described by its invariant phase space product, $EA\Omega$, where E is the energy, A is the area of the beam and Ω is the solid angle subtended by the electron beam envelope. The conservation of this phase space product is sometimes expressed as an emittance invariant, $\varepsilon_{\text{inv}} = r\alpha\sqrt{E} = (EA\Omega)^{1/2}/\pi$, where r is the radius of the beam and α is the half angle of the beam divergence. The phase space product of the polarized electron source must be less than that of the experiment or device to which it is coupled if the electron beam is to be accepted without loss. If the acceptance phase space of the device $(EA\Omega)_d$ is smaller than the phase space product of the source $(EA\Omega)_s$, the beam current is reduced by the ratio $(EA\Omega)_d/(EA\Omega)_s$. For an emitting area 0.5 mm in diameter, the emittance invariant of the NBS GaAs spin polarized electron source is estimated to be

$\varepsilon_{inv} = 6.5 \times 10^{-3}$ rad cm $eV^{1/2}$ (Pierce et al. 1980, Celotta and Pierce 1980). The emittance invariant could be further reduced by focusing the incident illumination to a smaller spot. The only polarized electron source with a smaller emittance invariant is a field emission source.

The energy distribution of the emitted electron beam is quite narrow and somewhat asymmetric. The photoexcited electrons are accelerated in the band bending region shown in fig. 2 (above). As hot electrons they can lose energy to optical phonons, which leads to an asymmetric distribution with a low energy tail. The energy full width at half the intensity maximum (FWHM) was measured to be 130 meV for the NBS source (Pierce et al. 1980) and 90–100 meV for different MBE photocathode surfaces (Alvarado et al. 1981a).

2.3. The quest for increased polarization

The 40–50% electron spin polarization attainable from NEA GaAs is quite adequate for many applications such as those described in sections 3 and 4. However, there are applications where the beam current cannot be increased to compensate for a less than 100% polarization due to beam-induced target damage. Alternatively, the maximum usable beam intensity may be constrained by space charge limitations in beam transport or limits on the maximum current that can be handled by a particular electron accelerator. In such situations, to improve the figure of merit P^2I of a source, only the polarization can be further increased. Because the signal rates in a high energy physics experiment are frequently low, it is not surprising that the impetus to achieve a 100% spin polarization, and thereby a fully optimized spin polarized electron source, has come from the high energy physics community.

What is wanted is a source with all the advantages of the GaAs source, such as high intensity and easy polarization reversal, but with 100% polarization. It can be seen from fig. 1, that the 50% polarization in GaAs is the result of two competing transitions, one that produces up and the other that produces down spins in the conduction band. It is appealing to consider the possibility of lifting the degeneracy at the top of the valence band so that electrons are excited to only one spin state. Degeneracy is lifted by reducing the symmetry of the crystal as, for example, by applying a uniaxial stress (D'yakonov and Perel' 1974) or by confining the electrons to quantum wells in one dimension in a semiconductor superlattice (Dingle et al. 1975). Luminescence measurements of the optical orientation in the conduction band, which is attained by lifting a degeneracy, can be a guide as to photoelectron spin polarizations which might be expected.

Under compressive stress, the light hole valence band ($m_j = \pm 1/2$) of GaAs is raised above the heavy hole ($m_j = \pm 3/2$) band. Theoretically, a maximum conduction band polarization $P_c = -0.8$ is expected for excitation from the light hole band with a stress at 90° to the propagation direction of the light

and $P_c = 1$ for a stress parallel to the light propagation direction. Luminescence measurements to determine P_c in the case of uniaxial compression perpendicular to the light directions show that values of P_c near the theoretical values are obtained (Berkovits et al. 1976, Zorabedian 1982). Luminescence measurements for compression parallel to the light axis are difficult because the light must pass through the stressing mechanism; photoemission measurements in such a geometry are extremely impractical. A possible exception to this is when the stress results naturally in the epitaxial growth of a GaAs layer on a substrate for which there is a lattice mismatch. There is a resulting compression or expansion of the GaAs lattice constants parallel to the interface and a corresponding expansion or compression of the lattice perpendicular to the interface, leading to a tensile or compressive uniaxial strain respectively. Strained layers with a mismatch of 1.5 to 2.5% can be grown with thicknesses up to a few hundred Ångstroms (Matthews and Blakeslee 1976, Osbourn et al. 1982). A disadvantage of stressing the GaAs to obtain a source of photoelectrons with higher P is that the splitting of the bands is only about 6 meV/kbar (Pollak and Cardona 1968). With maximum splitting of a few tens of meV, excitation would have to be from the low density of states region very near the band edge, resulting in low photoelectron intensities.

Another way to lift the valence band degeneracy is to confine the electrons and holes in one-dimensional potential wells. Superlattices of a series of GaAs wells separated by GaAlAs barriers have been fabricated. In this case the valence band is split a few tens of meV, depending on the superlattice geometry, with the heavy hole band on top. Luminescence measurements of such structures indicate an increase in conduction band polarization up to about 70% (Miller et al. 1979). Alvarado et al. (1981b) made such superlattices and measured the polarization of electrons that were photoemitted from them. A maximum polarization of 49% was observed. They attribute this to the fact that the highly polarized optically oriented electrons in the GaAs wells must be transported to the surface to be emitted; the transport is vanishingly small due to the low tunneling probability through the GaAlAs barriers. If electrons are excited with photon energy sufficient to raise them above the barrier, then electrons can be emitted from the GaAlAs barrier region itself and the polarization of these electrons is not enhanced. Superlattice structures tested so far are not suitable for a high polarization source, but there remains the possibility that structures of more suitable materials can be fabricated.

There exist materials in nature, the II–IV–V_2 compounds, with a chalcopyrite structure in which the valence band degeneracy is removed naturally by the lower crystal symmetry. These compounds are ternary analogs of III–IV compounds like GaAs which have the zincblende structure. The chalcopyrite unit cell is roughly that of zincblende doubled along a ⟨100⟩ direction which defines the c-axis. The group III element is alternately replaced by a group II and group IV element. There is a uniaxial compression along the c-axis that is

the main source of the crystal field that along with the spin–orbit splitting removes the valence band degeneracy, resulting in three separate doubly (spin) degenerate bands.

The problem with these materials is that they are not readily available in crystals large enough to be suitable for photocathodes. $CdSiAs_2$ is one of the most promising II–IV–V_2 compounds for a polarized electron source, and considerable effort is being made to grow the desired crystals (Sinclair 1981). The compression along the *c*-axis can be quite substantial. In $CdSiAs_2$, for example, it is about 7% of the lattice constant. This leads to a significant splitting of the valence bands, the difference between the first and second and between the second and third bands being 0.19 eV and 0.25 eV respectively (Shay and Wernick 1976, Kaufmann and Schneider 1974).

Optical transitions with σ^+ circularly polarized light to the conduction band minimum from the second valence band produce only down spins and from the third band produce only up spins; there are no allowed transitions with circularly polarized light from the uppermost valence band to the conduction band (Zürcher and Meier 1979). Thus, the natural compression along the *c*-axis causes splittings much greater than attainable by stressing GaAs. Furthermore, the light can be parallel to the compression axis, which is the stress configuration leading to maximum spin polarization. $CdSiAs_2$ has the basic characteristics which give it promise as a highly polarized electron source. Nevertheless, in addition to the crystal growing problem, there remain questions to be answered about such factors as the spin relaxation time and the possibility of lowering the vacuum level to a negative electron affinity or small positive electron affinity in order to extract the electrons excited to the states of proper symmetry in the lower most conduction band.

Very likely the maximum polarization in an optically oriented polarized electron source has not yet been achieved. The outlook for obtaining beams of higher polarization is promising.

3. *Polarization effects in electron–atom collisions*

3.1. *The "perfect" scattering experiment*

Polarized electron–atom scattering offers the opportunity to probe the fundamental spin-dependent interactions of importance in electron collision physics. Unlike scattering from surfaces or molecules, multiple scattering does not occur and the exchange and spin–orbit interactions can be studied for simple atomic systems. Even in this case, however, many approximations are necessary in the theoretical treatment, and it is the goal of experimental comparisons with theoretical models to test the validity of these approximate models.

This is best accomplished when every collision parameter is under control and the effect of varying each parameter can be separately observed. In conventional electron scattering experiments, the spin states of the target electrons and the incident electrons are random and all of the possible spin dependent effects must be averaged in the model as they are in the experiment. When polarization techniques are used to fully state select the target and incident electron quantum states a complete or "perfect" scattering experiment is possible (Bederson 1969, 1971, Wübker et al. 1982). Such experiments are qualitatively different from conventional scattering experiments in that the collision is fully characterized, and all the information that is theoretically possible to obtain about the collision is determined. The results of such experiments can be presented as quantum amplitudes and phases, rather than cross-sections. Since cross-sections are sums of squares of complex amplitudes, direct determination of the individual amplitudes themselves enhances the comparison with, and validation of, theoretical models.

The realization of "perfect" electron–atom scattering experiments has been a goal for many years. Such experiments have always presented formidable challenges because of the relatively small number of collision partners left after all of the state selection is performed and because of the inefficient methods required to select or detect specific states. The history of this field is therefore rich with the development of new techniques to produce intense, spin-selected atom or electron beams (Kessler 1976). Recently, optical pumping techniques have been very successfully applied both to the problem of producing an intense polarized electron beam (sect. 2) and to the problem of efficiently state selecting an atomic beam (Hertel and Stoll 1977). As a consequence, "perfect" scattering experiments now appear within reach.

The two most important interactions that can be probed are the spin–orbit and exchange interactions. A formalism that fully describes both effects, and their interaction, has been developed (Burke and Mitchell 1974, Khalid and Kleinpoppen 1983). However, each effect can be studied separately by using low-Z targets to minimize the spin–orbit coupling interaction or by using high-Z targets with no net spin orientation, so that exchange effects will be averaged over. "Perfect" scattering experiments that study exchange in elastic scattering are now under way, but many of the recent experiments (Baum et al. 1981, Hils et al. 1982, Alguard et al. 1977) have dealt with the experimentally less complex problems of the spin-dependence of near-threshold ionization as studied using a polarized atom beam and an incident polarized electron beam.

Studies of the spin–orbit interaction have progressed to the long sought-after point of obtaining a complete description of the scattering event. In a recent experiment, Wübker et al. (1982) have scattered a polarized electron beam from xenon atoms and observed the change in the electron polarization. The experimental arrangement is shown in fig. 3. A krypton-ion laser produces an

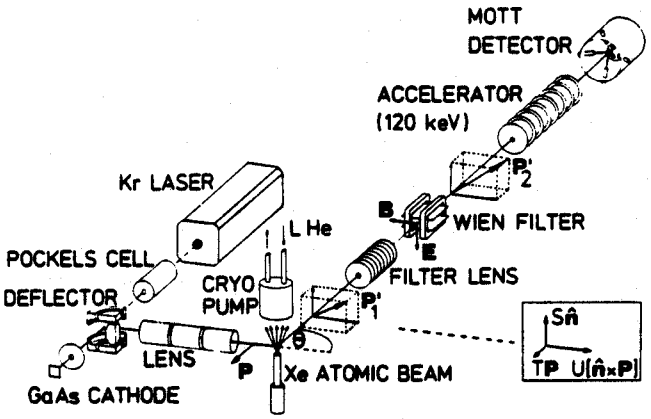

Fig. 3. Schematic of the polarized electron atom scattering apparatus. (From Wübker et al. 1982.)

intense photon beam which is given a modulated circular polarization on passing through a Pockels cell. The polarized electrons leave a GaAs photocathode at normal incidence with their polarization either parallel or antiparallel to the direction of travel. A 90° electrostatic deflector changes the direction of the beam without affecting the spin direction, resulting in a transversely polarized beam with polarization $\boldsymbol{P}$ as shown. After scattering the resulting polarization $\boldsymbol{P}_1'$ is given by

$$\boldsymbol{P}_1' = S\hat{\boldsymbol{n}} + T\boldsymbol{P} + U[\hat{\boldsymbol{n}} \times \boldsymbol{P}] \tag{4}$$

where S, T, and U are functions of the complex direct scattering amplitude, $f(E,\theta)$, and spin-flip scattering amplitude, $g(E,\theta)$. The orientation of the three components of polarization is shown in the insert. The purpose of the electron optics, Wien filter, and Mott detector following the collision region is to determine the magnitude of each of the three final polarization components. Since the Mott scattering process (Kessler 1976) can only measure two at a time, the Wien filter is used to select which components are measured.

Over an energy range of 30–360 eV, Wübker et al. were able to fully determine S, T, and U, as shown in fig. 4. Also shown are two different theoretical approximations. The encouraging agreement seen at higher energies vanishes at lower energies. This data has also been presented in terms of $|f|$, $|g|$, and ϕ, the phase difference between f and g (Wübker et al. 1982), the overall phase being arbitrary.

Experimental investigations of exchange scattering using GaAs sources and polarized alkali beams are being actively pursued in a number of laboratories. We can look forward to the results of these "perfect" scattering experiments during the next few years.

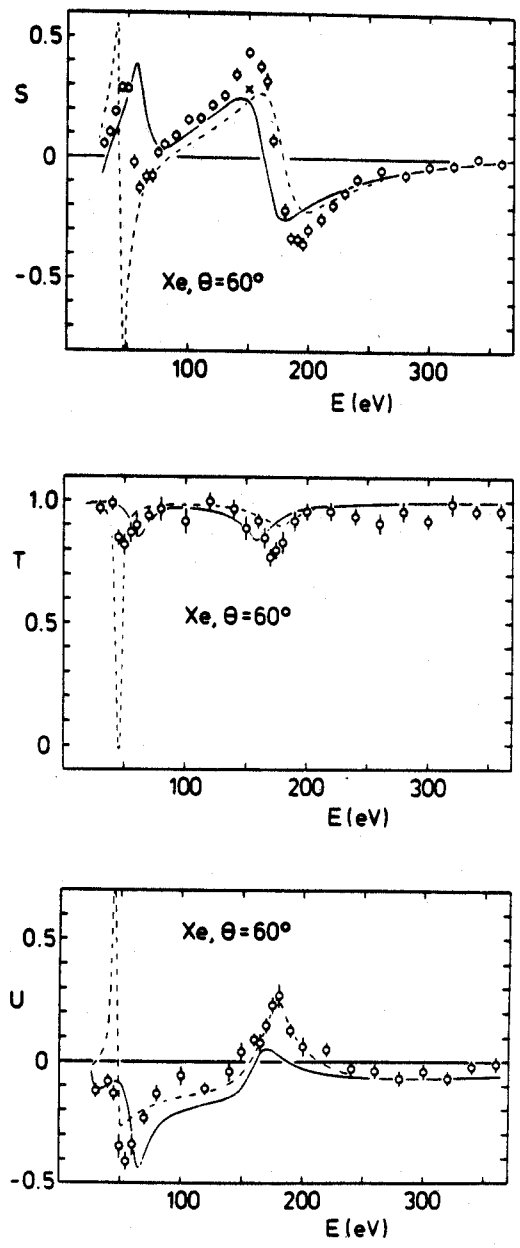

Fig. 4. Energy dependence of the parameters S, T, and U at a scattering angle of $\theta = 60°$. Experimental points have one sigma error bars. Theoretical curves: relativistic calculations including exchange (solid curve) and charge-cloud polarization plus exchange (dashed curve). (From Wübker et al. 1982.)

3.2. Optical orientation for spin polarization analysis

An additional application of "optical pumping" should be mentioned with regard to atomic physics studies of polarization phenomena. While we have so far concentrated on the conversion of circularly polarized light into a net polarization of an electron beam, the inverse process is also of great utility. Can an electron polarization detector be made in which a polarized beam collides with a substance and gives up its angular momentum, which then appears as a circular polarization of the emitted light? Eminyan and Lampel (1980) demonstrated that this is possible in an experiment where polarized electrons produced with a GaAs source are collided with an atomic zinc beam. They observed the polarization of light emitted following the excitation from the $4s^2\,^1S_0$ ground state to the $4s5s\,^3S_1$ excited state. This excitation is accomplished via the exchange of electrons with opposite spins, and results in the transfer of a unit of angular momentum. This causes a nonuniform population because a spin up incident electron, for example, can not populate the $|^3S; S=1, M_s=-1\rangle$ substate. The resulting substate populations are:

$$N(M_s=0)=1/3, \qquad N(M_s=\pm 1)=1/3 \quad (1\pm P), \tag{5}$$

where P is the incident electron polarization. The decay of this state to the $4s4p\,^3P_J$ states allows the determination of the electron polarization from the polarization of the emitted light. Unlike the Mott polarization detector, this method permits the analysis of both the transverse and the axial polarization.

4. Polarized electron scattering studies of surface magnetism

4.1. Spin-dependent interactions

Electron spectroscopy has proven to be very powerful in elucidating the properties of solids. Electron spectroscopy is generally quite surface sensitive, that is, the electrons probe only the outer few layers of the solid. The origin of this surface sensitivity lies in the strong electron–electron scattering which leads to mean free paths of less than 10 Å for electrons with energies from 10 eV to a few hundred eV.

Many electron spectroscopies can now be made spin dependent by using a spin polarized electron beam from optically oriented GaAs. The important terms of the interaction Hamiltonian for spin dependent scattering can be written

$$H=V(r-r_i)+\frac{1}{2m^2c^2}\,\frac{1}{(r-r_i)}\,\frac{\mathrm{d}V(r-r_i)}{\mathrm{d}r}\,s\cdot L+\sum_i J(r-r_i)\,s\cdot S_i, \tag{6}$$

where r is the position of the incident electron with spin s and angular

momentum L, r_i is the position of the ith atom with spin S_i, and $J(r - r_i)$ is the exchange coupling constant. The first term is the spin independent scattering potential, the second is the spin–orbit scattering potential, and the third is the spin dependent part of the exchange potential.

When a polarized electron beam is scattered from high atomic number elements there is a substantial spin dependent interaction due to the spin–orbit interaction. This interaction has been used to determine atomic structure at surfaces by polarized low energy electron diffraction (PLEED) (Feder 1981, Pierce and Celotta 1981). Further, the spin dependence of the interference fine structure observed in low energy electron scattering (McRae et al. 1981, Pierce et al. 1981) has been used (Jennings and Jones 1982, Jones and Jennings 1983) to determine the shape of the electronic potential barrier at a surface.

An important application of the GaAs polarized electron source is to the study of surface magnetism. The spin dependent signal results from the exchange interaction between an electron spin s in the polarized incident beam and the oriented spins S_i at the surface of a ferromagnet. In this section we will discuss the results of a few experiments which have exploited optically oriented GaAs as a source of polarized electrons to study surface ferromagnetism.

4.2. Apparatus

The three basic elements of an apparatus to investigate surface magnetism with a polarized electron beam are the source of polarized electrons, the magnetic target, and a means to monitor the interaction by detecting, for example, the scattered electrons or possibly photons that might be produced. The electrons that are photoemitted from the optically oriented GaAs are formed into a beam that is appropriate for the particular experiment. For a diffraction experiment, a well collimated beam is wanted at the sacrifice of some intensity. On the other hand, for an inverse photoemission experiment high intensity is of primary importance.

The target must be magnetized to align the domains as the area sampled by an electron beam typically covers several domains. It is also desirable to be able to reverse the magnetization to discriminate against non-magnetic effects. A suitable means to magnetize a sample is by a C-shaped electromagnet as shown in fig. 5. The sample acts as the "keeper" of the electromagnet and there is a minimum of stray field in this closed magnetic circuit. The sample is magnetized by applying a current pulse to the coil, and held in saturation by the remanent magnetization of the iron electromagnet (Pierce et al. 1982). For some applications, such as measuring surface hysteresis curves, the contribution of the iron core obscures the measurement. This can be avoided by making the magnetic circuit of the same material as the sample; this was accomplished in measurements of ferromagnetic glasses by forming the ribbon into a loop and clamping the overlapping ends (Unguris et al. 1984). In the

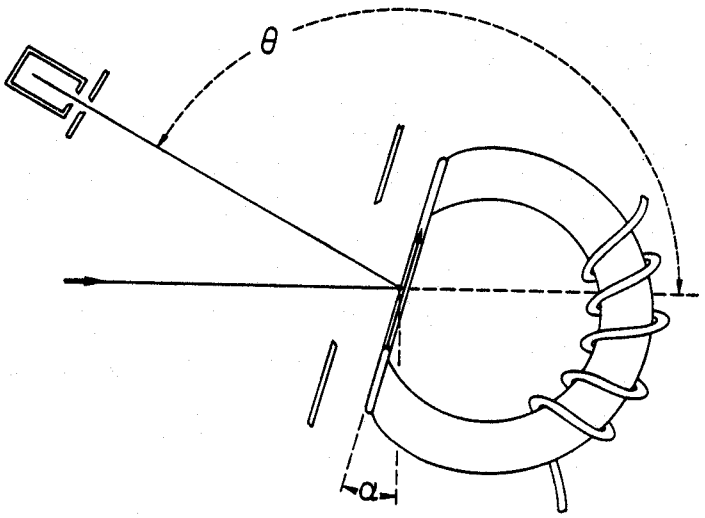

Fig. 5. Schematic of the polarized electron scattering geometry. Sample and electromagnet form a closed magnetic circuit and can be rotated about an axis in the sample surface perpendicular to the plane of the figure to vary the angle of incidence α. Scattering angle θ is determined by the position of the scattered electron detector relative to the direction of the incident electron beam. (From Pierce et al. 1982.)

case of single crystals, the ideal solution is a rectangular "picture frame" geometry as used in the polarized electron scattering studies of Alvarado et al. (1982a, b). Another technique which is appropriate, especially for thin samples, is simply to magnetize (pole) the sample along an easy magnetization direction (Kisker et al. 1980). There is no magnetic material to complete the magnetic circuit but the stray fields may be sufficiently small for thin samples in favorable geometries.

For the third element of the experiment, the detection of the spin dependent signal, different methods have been used. Perhaps the simplest is to monitor the current absorbed by the sample as the polarization of the incident beam is alternately parallel or antiparallel to the magnetization (Siegmann et al. 1981). More information is obtained if the scattered intensity is measured at a particular scattering angle, again for the incident beam polarization respectively parallel or antiparallel to the magnetization. Electron energy analysis is employed to discriminate between elastically or inelastically scattered electrons. In the studies discussed below of the temperature dependence of surface magnetism, the spin dependent asymmetry of the elastically scattered electrons was detected using a retarding field analyzer and a Faraday cup (Pierce et al. 1982) and a hemispherical energy analyzer with an electron multiplier (Alvarado et al. 1982a, b). One mechanism of inelastic scattering of electrons is

a radiative transition in which ultraviolet photons are emitted. This process, known as "inverse photoemission", has been observed using a polarized electron beam from optically oriented GaAs and a Geiger–Müller counter to detect the photons as described later in this section. We note that the polarized electron source can also be used in combination with a spin analyzer to measure changes in the electron polarization on scattering (Ravano et al. 1982) but such measurements will not be discussed here.

4.3. *Surface hysteresis curves*

As a first example of application of an optically pumped GaAs spin polarized electron source to study surface magnetic properties we consider the normalized asymmetry A in the scattered intensities $I_\uparrow$ and $I_\downarrow$, defined as

$$A = (1/|P_0 \cos\alpha|)(I_\uparrow - I_\downarrow)/(I_\uparrow + I_\downarrow), \tag{7}$$

where $I_\uparrow$ and $I_\downarrow$ are, respectively, the scattered intensities for the effective incident polarization component $P_0 \cos\alpha$ parallel and antiparallel to the majority spin direction in the target. Equivalently, $I_\uparrow$ and $I_\downarrow$ correspond to the scattered intensities when the electron magnetic moments of the incident beam are respectively parallel and antiparallel to the sample magnetization. The angle α is that between the incident spin polarization and the spins in the surface. The scattering asymmetry A is readily measured because the spin polarization of the electron beam from a GaAs source is easily and rapidly reversed. The denominator of eq. (7) is proportional to the d.c. part of the scattered intensity while the numerator is proportional to the a.c. part of the scattered intensity in phase with the polarization modulation and is easily detected with a lock-in amplifier.

The variation of the asymmetry A with applied magnetic field, shown in fig. 6, is a hysteresis curve of the surface magnetization, in this case for the ferromagnetic glass $Fe_{8.15}B_{14.5}Si_4$ (Unguris et al. 1984). The shape of the hysteresis curve depends sensitively on the condition of the sample surface. Before the surface was cleaned by Ar ion bombardment sputtering, Auger analysis indicated the presence of a surface oxide and no asymmetry was measured. Initial sputtering removed most of the oxide, resulting in the hysteresis curve of fig. 6a. Prolonged sputtering such that about 500 Å of material were removed, and no change was observed on further sputtering, left a surface which produced the hysteresis curve of fig. 6b. Annealing the sample for one minute at 120°C produced the square hysteresis curve shown in fig. 6c without altering the surface composition as monitored by Auger spectroscopy. This dramatic effect of annealing is presumably the result of removing ion bombardment induced strains in the surface of the material. The sensitivity of the electron scattering to the magnetic properties of the outer few atomic layers is striking. In contrast, hysteresis curves measured with the magneto-optic Kerr

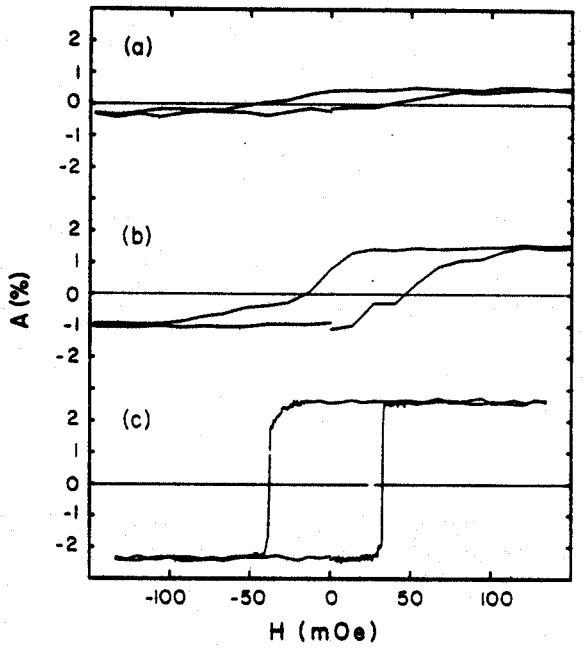

Fig. 6. Surface hysteresis curves, measured using 110 eV electrons at $\theta = 166°$, shown during various stages of sample preparation: (a) after initial sputtering which was just sufficient to remove the oxide layer; (b) after prolonged sputtering; (c) after annealing to 120°C for 1 min. (From Unguris et al. 1984.)

effect produced square hysteresis curves, as in fig. 6c, for all sample preparations, including the oxide coated surface. This is because the optical measurement probes a depth of 150 Å compared to approximately 2.5 Å estimated for our elastic polarized electron scattering hysteresis curves. This estimate is based on a mean free path for inelastic scattering of $\lambda = 5$ Å for 100 eV electrons; the electrons travel, on the average, $\lambda/2$ into and out of the sample.

The scattering asymmetry A shown in fig. 6 is proportional to the surface magnetization. While this is frequently the case, it need not be so in general (Feder and Pleyer 1982). However, from symmetry we know that

$$A = \alpha M_s + \beta M_s^3 + \gamma M_s^5 + \cdots . \tag{8}$$

In the case of scattering from a ferromagnetic glass, Pierce et al. (1982) found that in the backscattering direction single scattering is dominant; an upper limit of 30% was placed on multiple scattering which could lead to the higher-order terms in eq. (8). When there is only single scattering, $A \propto M_s$ at all temperatures. Thus, a ferromagnetic glass is ideal for measuring the temperature dependence of the surface magnetization. In a single crystal where

electrons are diffracted and multiply scattered, it is not clear which term of eq. (8) is dominant in a diffraction spot, but it can be argued that $A \propto M_s$ as $T \to T_c$ (Feder and Pleyer 1982). Hence, magnetic single crystals are suitable for tests of the temperature dependence of the surface magnetization near the Curie temperature.

4.4. *Temperature dependence of surface magnetization*

At low temperatures, the ratio of the bulk magnetization at a temperature T, $M_b(T)$, to the bulk magnetization at zero temperature, $M_b(0)$, follows the **Bloch law**

$$M_b(T)/M_b(0) = 1 - B_b T^{3/2} + \cdots . \tag{9}$$

The constant B_b is characteristic of the low temperature, long wavelength spin waves or magnons. At a surface, the boundary conditions are different and the deviation of the spontaneous magnetization at a temperature T from its zero temperature value can be different than in the bulk. Assuming that standing spin waves have antinodes at the surface, Rado (1957) predicted that the surface magnetization would decrease as $T^{3/2}$ but with a value B_s twice as large as the bulk value B_b. A more extensive calculation of Mills and Maradudin (1967) included both surface and volume spin waves. They found that the surface spin wave contribution is exactly cancelled by a reduction in the bulk spin wave contribution such that the same result as the earlier calculation is obtained, namely that the temperature dependence is as $T^{3/2}$ and $B_s = 2B_b$.

These theories were tested for the first time by measuring the spin dependent scattering asymmetry of a polarized electron beam originating from an optically pumped GaAs polarized electron source. When the scattering asymmetry as a function of temperature was plotted against the bulk magnetization at the same temperatures a straight line was obtained confirming that the surface magnetization varies with the same power of the temperature as does the bulk magnetization; in this temperature range that is as $T^{3/2}$ to a very good approximation. The surface magnetization as measured by spin polarized electron scattering from a ferromagnetic glass, $Ni_{40}Fe_{40}B_{20}$, is plotted as a function of temperature in fig. 7 along with the measured bulk magnetization. Electrons with an energy of 90 eV were scattered through an angle $\theta = 166$ and the data points represent $(A^+ + A^-)/2$ where A^+ and A^- are the scattering asymmetries for two opposite magnetization directions, thereby eliminating residual apparatus induced asymmetries. The surface magnetization is seen to fall more rapidly than the bulk. The dashed line is a $T^{3/2}$ fit to the data from which the coefficient B_s was determined to be about three times as large as B_b, in only approximate agreement with the theoretical prediction. The discrepancy might be due to the simplifications of the theory to an idealized

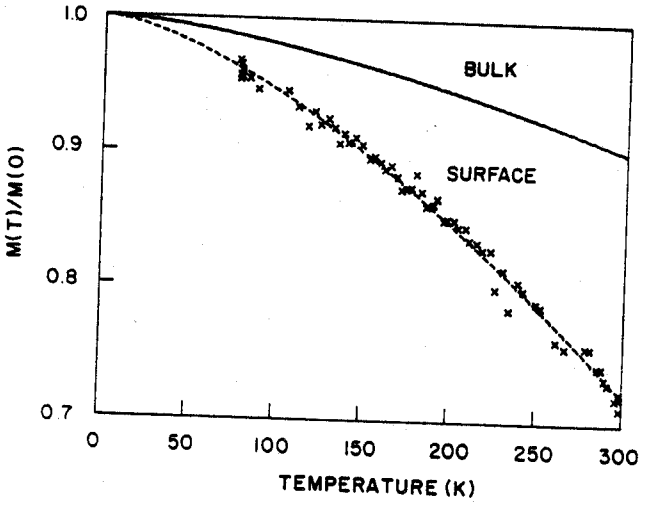

Fig. 7. Spin polarized electron scattering is used to determine the difference in the temperature dependence of the magnetization at the surface of a ferromagnetic glass, $Ni_{40}Fe_{40}B_{20}$, from that of the bulk. (From Pierce et al. 1982.)

Heisenberg ferromagnet. If either the magnitude of the magnetic moment at the surface or its exchange coupling to the bulk is reduced compared to the bulk values, it would be easier to excite spin waves at the surface and hence lead to a larger B_s. It is interesting to note that the theories of Rado and of Mills and Maradudin had to wait 25 and 15 years respectively to be tested experimentally. The application of the optically oriented polarized electron source provided the qualitative difference in making such surface magnetization measurements feasible.

The critical behavior of the surface magnetization of the Ni(100) and Ni(110) surfaces has been measured by Alvarado et al. (1982a, b) using polarized low energy electron diffraction (PLEED). The spin dependent asymmetry of the elastically scattered electrons in a PLEED beam was measured in a temperature region near the Curie temperature T_C. Here the surface magnetization is expected to vary as

$$M_s(T) \propto (1 - T/T_C)^{\beta_1}, \tag{10}$$

where β_1 is the critical exponent to be determined. The incident electron beam was obtained from an optically pumped GaAs source using $Al_{0.37}Ga_{0.63}As$ as the photocathode and a HeNe laser as the light source. The target was in the picture frame geometry. The magnetization could be reversed by a current pulse in the coil around one arm of the picture frame. The sample temperature was varied in the range $0.002 \leq (1 - T/T_C) < 0.1$ by indirect heating by a pulsed tungsten heater which was off during the measurement.

The critical exponent is determined from the graph of the scattering asymmetry versus reduced temperature shown in fig. 8. Spin–orbit and apparatus asymmetry contributions are removed by plotting $(A^+ + A^-)/2$. The scattering asymmetry A is proportional to $M_s(T)$ in this region so that β_1 can be determined directly from the slope of the curve in fig. 8. Three different PLEED beams were measured for the (100) surface and two for the (100) surface, giving values for β_1 of 0.80 ± 0.02 and 0.79 ± 0.02 respectively (Alvarado et al. 1982b). The values were independent, within experimental uncertainty, of the kinetic energy or angle of incidence of the polarized electron beam. The experimental values for β_1 are somewhat smaller than the predictions of calculations for the Heisenberg model which range from 0.81 to 0.88. These measurements of the surface magnetic critical behavior are an elegant application of an optically pumped polarized electron source and represent the first of what is expected to be a growing number of measurements of the magnetic critical behavior of semi-infinite systems.

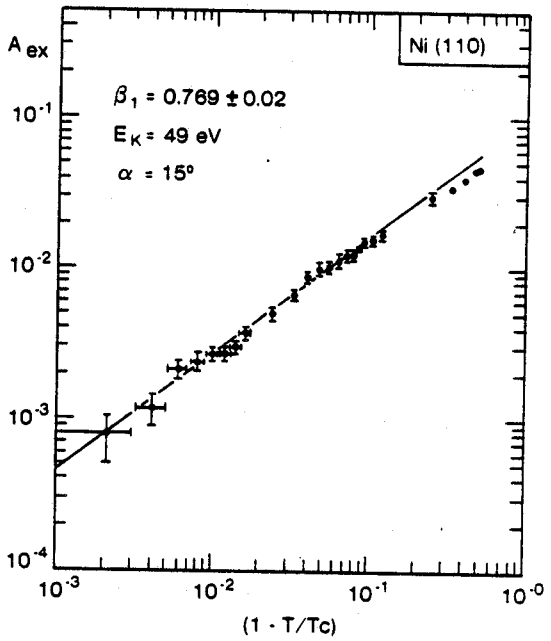

Fig. 8. The temperature dependence of the magnetic exchange scattering asymmetry for specular scattering from Ni(110) at an angle of incidence $\alpha = 15°$ in the neighborhood of the Curie temperature. The slope determines the critical exponent β_1 of the surface magnetization. (From Alvarado et al. 1982b.)

4.5. Spin polarized inverse photoelectron spectroscopy (SPIPES)

Photoemission spectroscopy has developed as a powerful technique to determine the electronic structure of solids. Angle resolved photoelectron spectra contain information which allows one to map out the band structure of occupied electron states. Instead of measuring the kinetic energy of photoemitted electrons excited by incident photons at a particular energy, one can do the inverse and vary the energy of an incident electron beam and measure the number of photons emitted at a particular energy. This is called bremsstrahlung isochromat spectroscopy or inverse photoemission spectroscopy (Dose 1977). Inverse photoemission has the important advantage that it allows the investigation of unfilled electronic states between the Fermi level and the vacuum level, a range inaccessible to ordinary photoemission measurements. The inverse photoemission experiment is also angle resolved when the incident electrons are in a well defined beam (Woodruff and Smith 1982).

Moreover, if the incident electron beam is polarized and contains, for example, only spin up electrons, then photons are emitted only when there are spin up final states for the electron to drop into. Thus by measuring the photon intensity in phase with the polarization reversal of the incident beam, the spin character of the unfilled electronic states can also be determined. The unfilled states or d-holes that give rise to the ferromagnetism in transition metals can now be studied directly by spin polarized inverse photoelectron spectroscopy (SPIPES). We describe here the first such SPIPES measurements; they were made on a Ni(110) surface by Unguris et al. (1982).

Nickel is a 3d ferromagnet which provides an ideal test case for SPIPES. The d-bands are exchange split into two spin sub-bands, the filled "majority" spin bands and the partially filled "minority" spin bands. In Ni, the d-holes are thought to extend only a few tenths of an eV above the Fermi level and to be of entirely minority spin character. Thus a measurement of the photon intensity when the polarization of the incident beam is in the minority ($\downarrow$) spin direction should produce a peak at the Fermi level while no peak is expected for majority ($\uparrow$) spin electrons.

A schematic of the inverse photoemission apparatus is shown in fig. 9. Only the detector has been changed compared to fig. 5, from an electron detector to a photon detector. Compared to previous inverse photoemission experiments (Woodruff and Smith 1982) the distinguishing feature of this apparatus is the spin polarized electron beam from optically oriented GaAs. The photons which are produced when the polarized incident electrons lose energy and fall into empty states are detected by a Geiger–Müller counter. It is filled with iodine and helium and has a peak sensitivity at 9.7 eV and a band pass of 0.7 eV (Denninger et al. 1979). The low energy cutoff is determined by the ionization threshold of the iodine and the high energy cutoff by the transmission of the

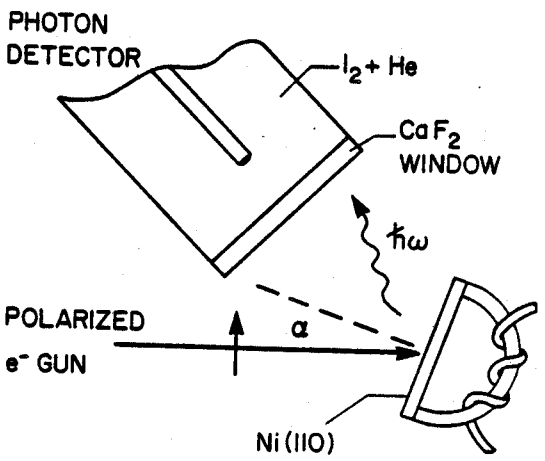

Fig. 9. Schematic of the apparatus for angle-resolved, spin polarized inverse photoelectron spectroscopy. (From Unguris et al. 1982.)

CaF_2 window. This photon detector is placed close to the interaction region as shown in fig. 9 so as to subtend the maximum solid angle and collect the most photons. A spectrometer which allows the detected photon energy to be selected can also be used but the signal is much reduced due to the smaller solid angle (Fauster et al. 1983).

The results of the first angle resolved SPIPES measurements are shown in fig. 10 for two angles of incidence, $\alpha = 0°$ and 20°. The peak observed in the $N_\downarrow$ spectra is absent in the $N_\uparrow$ spectra. Note that the spectra were obtained by varying the energy of the incident electron beam; the energy axis is that of the final state with respect to the Fermi level. The band structure diagram at the right shows the energy levels for electrons moving perpendicularly to the (110) surface. The arrow shows a radiative transition to a minority d-hole state that gives rise to the peak in the $N_\downarrow$ spectrum. The increased intensity in the $N_\downarrow$ peak in going from normal incidence to $\alpha = 20°$ is due to selection rules for the optical transitions. There is also a slight dispersion of the $N_\downarrow$ peak to lower energy with increasing angle of incidence. The main features of the SPIPES results – the minority spin character of the peak, the intensity variation and energy dispersion of the peak – can all be understood in terms of the Ni band structure.

It is expected that these initial experiments on a well known system will be extended to less well known systems or to the case of adsorbates on a ferromagnetic surface; this should provide important information about the role of d-holes in chemisorption. In contrast to the elastic scattering studies we described earlier in this section, which determined the hysteresis curve of the

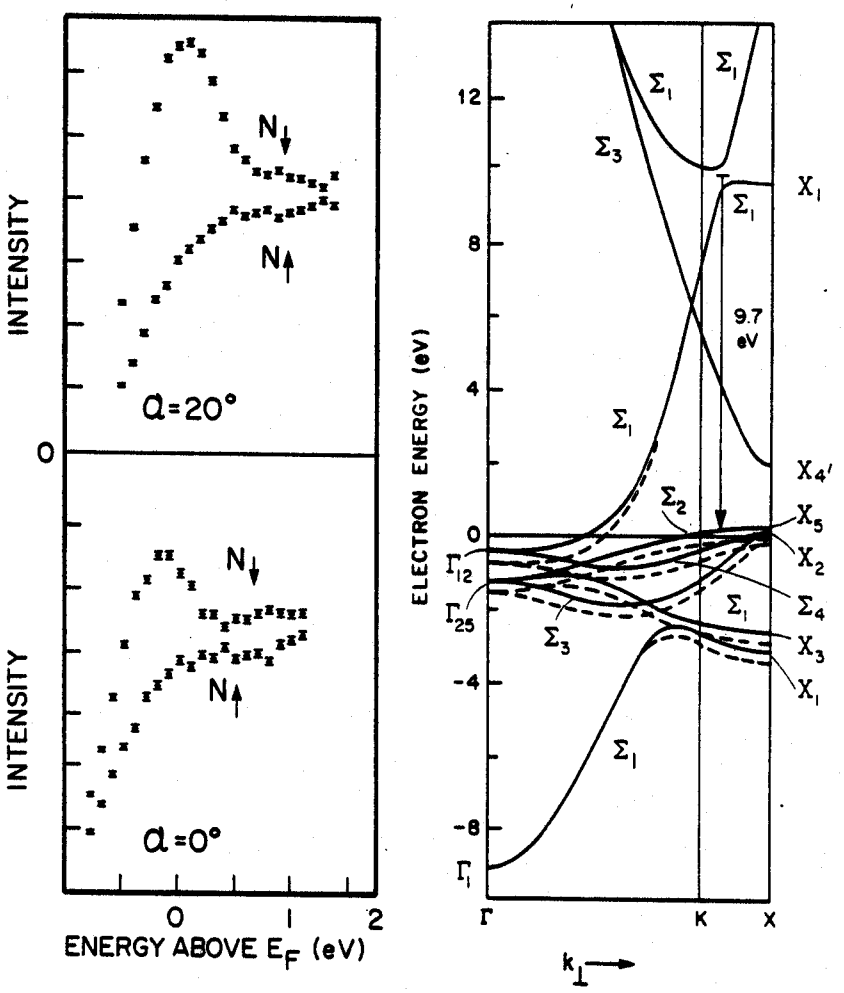

Fig. 10. The photon intensities $N_\uparrow$ and $N_\downarrow$, generated by incident polarized electrons with spins respectively in the majority and minority spin directions is shown at the left for two angles of incidence. On the right is the band structure along the ΓKX line corresponding to normal electron incidence on Ni(110). Dashed and solid lines represent majority and minority spin bands respectively. The arrow shows a possible radiative transition at $\hbar\omega = 9.7$ eV to minority spin final states just above E_F; such transitions give rise to the large $N_\downarrow$ peak in the measured spectra. (From Unguris et al. 1982.)

surface magnetization and the temperature dependence of the surface magnetization, inelastic scattering with detection of the radiative transition, i.e., SPIPES, determines the spin dependent electronic structure of the unfilled states that give rise to the surface magnetization.

5. *Parity non-conservation in high energy inelastic electron scattering*

The use of optical orientation to obtain spin polarized electrons in photoemission from GaAs was a key element in a series of elementary particle physics experiments (Prescott et al. 1978, 1979). Longitudinally polarized, high energy electrons (16.2 GeV $< E_0 <$ 22.2 GeV) were scattered inelastically from unpolarized deuterium or hydrogen targets. The energy of the scattered electrons ranged from 10.2 to 16.3 GeV. If parity is conserved in the inelastic scattering process, the number of electrons scattered should be independent of the direction of the longitudinal polarization or helicity of the incident electrons. Parity violating effects as the result of weak neutral currents are predicted in many unified gauge theories.

The experiment was designed to detect a very small parity violating asymmetry A which is given by

$$A = (\sigma^+ - \sigma^-)/(\sigma^+ + \sigma^-), \tag{11}$$

where σ^+ (σ^-) is the inelastic scattering cross-section $\mathrm{d}^2\sigma/\mathrm{d}\Omega\,\mathrm{d}E'$ for positive (negative) helicity electrons. (Positive helicity corresponds to electron spin in the direction of electron momentum.) The asymmetry is expected in the quark–parton model to be proportional to the magnitude of the four-momentum transfer squared, Q^2, and a function of the fractional energy loss, $y = (E_0 - E')/E_0$,

$$A = Q^2\left\{a_1 + a_2\left[1-(1-y)^2\right]/\left[1+(1-y)^2\right]\right\}. \tag{12}$$

The coefficients a_1 and a_2 are constants for deuterium and are related to the neutral current couplings of the electron and the quarks. Measurements as a function of y allow the determination of a_1 and a_2 which are predicted to have different values in different gauge theories.

The parity violating asymmetries predicted by various theories are very small, of order $10^{-4}Q^2$ for the kinematics of the SLAC experiment. Parity violating asymmetries could not be observed in earlier experiments with muons (Bushnin et al. 1976) and electrons (Alguard et al. 1976, Atwood et al. 1978). The accuracy in the electron experiment, for example, only allowed for upper limits of 2×10^{-3} and 7×10^{-3} for Q^2 values of 1.2 and 4.2 $(\mathrm{GeV/c})^2$, respectively, to be placed on the asymmetry. In their initial experiments,

Prescott et al. (1978) found an asymmetry $(-9.5\times10^{-5})Q^2$ at $Q^2=1.6$ $(\mathrm{GeV}/c)^2$ and $y=0.21$. The first observation of a parity violating asymmetry in deep inelastic electron scattering arising from the interference of the electromagnetic current and weak neutral current was truly a landmark experiment (Lubkin 1978). Already it could rule out certain classes of gauge theories which predicted no observable parity violation. Subsequent experiments as a function of y allowed further distinction between theoretical models.

5.1. Special features of the SLAC polarized electron source

Prescott et al. (1978) stated "of crucial importance to this experiment was the development of an intense source of longitudinally polarized electrons." The GaAs spin polarized electron source developed at SLAC for these high energy experiments (Sinclair et al. 1976) differed in several respects from the sources described earlier in this chapter. A schematic of the polarized electron source is shown in fig. 11. The GaAs photocathode is clamped to a molybdenum block

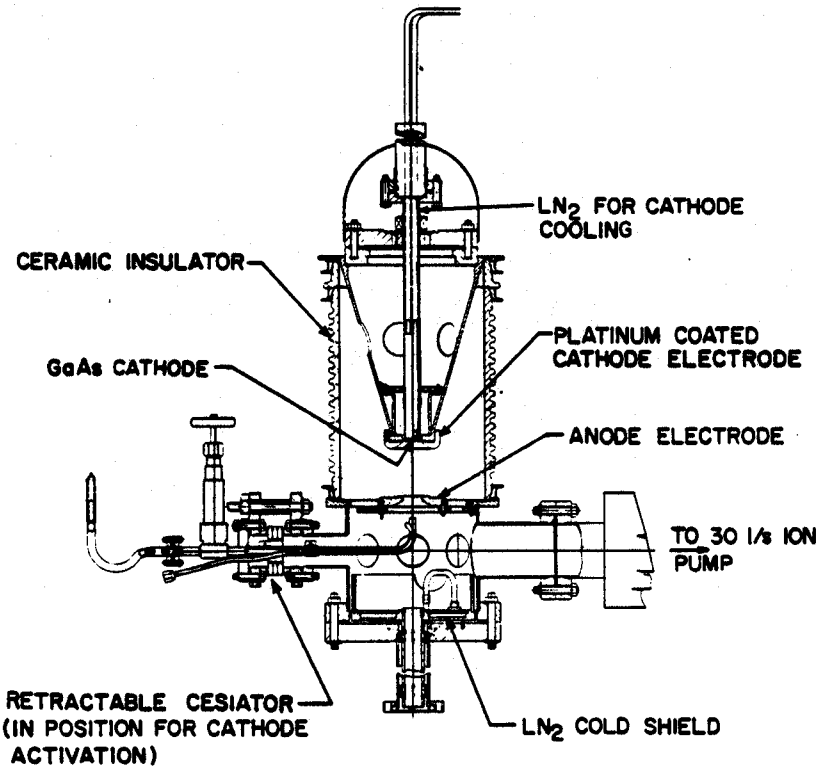

Fig. 11. Schematic of the SLAC GaAs polarized electron source. The cathode is at a potential of −70 kV suitable for injection into the linear accelerator. (Courtesy C.K. Sinclair.)

which is supported from a large ceramic insulator. The cathode was at a potential of -70 kV to provide the 70 keV electrons required for injection into the linear accelerator. Careful engineering was required to operate at these high voltages. For example, the platinum coating on the cathode electrode around the GaAs has a high work function which inhibits high voltage breakdown. Cesium deposits on the insulator can also cause breakdown and had to be avoided. The photocathode was at liquid nitrogen temperature in operation and a polarization of 37% was obtained. In fig. 11, there is a LN_2 cold shield so that the cathode could only "see" a cold surface. This was found to increase the lifetime of the cathode by decreasing the contaminants reaching the photocathode. Cathode intensity lifetimes in excess of 24 h were achieved. This polarized electron source was extremely reliable, operating on a 24 hour-a-day basis for six weeks with a long term average beam availability of 93% (Sinclair 1981).

A flash pumped dye laser operating at a wavelength of 710 nm caused the optical orientation and emission of polarized electrons from the GaAs photocathode. The laser produced 1.5 μs pulses at the rate of 120 pulses per second, appropriate for the linear accelerator. The linearly polarized light from the laser was converted to circularly polarized light by a Pockels cell, which produces a phase retardation proportional to the voltage applied to the birefringent crystal. The helicity of the photons and, hence, that of the polarized electrons, could be rapidly reversed by reversing the voltage on the Pockels cell. A calcite prism was used to rotate the plane of polarization of the light incident on the Pockels cell from $\phi = 0°$ to 90° where $\phi = 0°$ corresponded to positive (negative) helicity electrons produced by a positive (negative) Pockels cell voltage. This provided a test for systematic errors in the experiment, such as beam intensity variations that might be introduced by the Pockels cell. An example of such a test is given in fig. 12 where the measured asymmetry changes sign as ϕ varies from 0 to 90° and is consistent with zero as it should be for $\phi = 45°$ where unpolarized electrons are produced.

Two features of the GaAs spin polarized electron source were essential to the success of the SLAC parity violation experiment: (1) the high intensity polarized electron beam that could be achieved, and (2) the ability to rapidly reverse the electron beam helicity. With regard to both of these factors, the GaAs source offered significant advantages over previously used sources. Beam intensities at the target of 1 to 4×10^{11} electrons/pulse were achieved. The particle flux to the detectors using the GaAs source was so high that individual particles were not counted. Rather the total charge was integrated over each pulse and typically corresponded to one thousand electrons per 1.5 μs pulse. Even with this high scattered flux, to measure an asymmetry of 10^{-5} with one standard deviation requires on the order of 10^{10} events and hence about one day with a beam pulse rate of 120 per second or $\sim10^7$ per day. The high intensity of the polarized beam from the GaAs source was clearly important

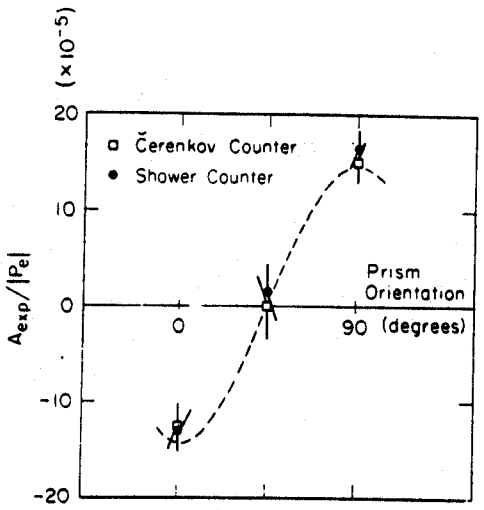

Fig. 12. The experimental asymmetry measured for different orientations of the calcite prism, and hence different beam helicities, shows the expected variation (dashed line). (From Prescott et al. 1978.)

for this experiment. In fact, the several hundred mA currents that could be obtained from the cathode were more than could be utilized. At such currents the transport from the source to the accelerator was space charge limited. The accelerator can accept up to about 80 mA; higher currents load the accelerator and cause an unwanted energy variation (Sinclair 1981).

The ability to rapidly change the helicity of the electron beam from the GaAs source was used to advantage in the SLAC experiment to minimize systematic effects. The random reversal of the polarization on a pulse-to-pulse basis avoided the possibility of the electron helicity changing synchronously with changes in any experimental parameter. Any effects of periodic fluctuations of experimental parameters would tend to be averaged out. Not only the speed of polarization reversal, but the stability in intensity and beam position on polarization reversal of the SLAC GaAs source was important.

5.2. Experimental layout

A schematic of the layout of the experiment is shown in fig. 13. Electrons from the GaAs polarized electron source or the conventional electron gun could be accelerated by the two-mile long linear accelerator to the target which consisted of a 30 cm long cell of liquid deuterium. Electrons which were scattered inelastically at 4° were momentum analyzed and focused by the spectrometer. The electrons were detected in lead-glass shower counters (TA) and a gas

Čerenkov counter (C). The same electrons were collected in each counter so data points such as those shown in fig. 12 were not statistically independent. However, since the two types of detectors are expected to respond differently to potential backgrounds, the consistency of the data from the two counters showed that such backgrounds were small. The spin polarization of the accelerated electrons was measured by scattering from a magnetized foil, known as Møller scattering (Bincer 1957, Ford and Mullin 1957). Møller scattering was used previously (Cooper et al. 1975) to determine that the accelerated beam maintains its polarization, and was used in this experiment to measure the average beam polarization of 37%.

Also indicated in fig. 13 is a system to monitor the beam current, energy, position, and angle, all parameters which could affect the measured yield of scattered electrons. Any systematic variation of these parameters with the variation of electron helicity would lead to a false asymmetry. These quantities were measured precisely on a pulse-to-pulse basis and used with a microcomputer driven feedback system to stabilize the average beam energy, position, and angle. This measurement of the size of the helicity dependent differences in beam parameters was used to correct the measured asymmetry. The size of such corrections, $\sim 2.5\%$ of A, were included in the systematic error given for the asymmetry measurement.

5.3. *Results*

Several checks were made to test that the measured asymmetry was the result of the electron beam helicity and that no asymmetry was measured for an unpolarized beam. One of the null tests was discussed in connection with fig. 12 which shows that unpolarized electrons, which are produced when linearly polarized light strikes the GaAs, do not cause a scattering asymmetry. Like-

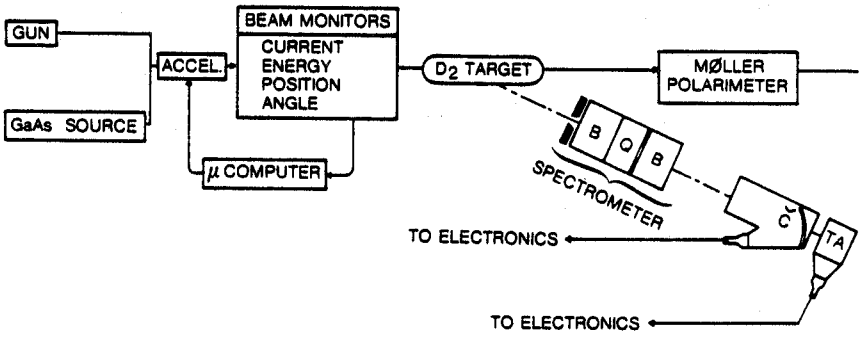

Fig. 13. Schematic of the experiment to test parity non-conservation in high energy inelastic electron scattering. (From Prescott et al. 1978.)

wise, no asymmetry was observed using the unpolarized electron beam from the regular SLAC electron gun. Random fluctuations in the beam parameters were found to be small compared to the 3% pulse-to-pulse fluctuations in the counting statistics. Another test takes advantage of the fact that the polarization of the incident electron beam is energy dependent (Cooper et al. 1975) because of the precession of the polarization in the magnetic field used to bend the accelerated beam by 24.5° into the experimental area. The precession, θ_p, is due to the anomalous magnetic moment, $g-2$, of the electron and is given by $\Theta_p(\text{rad}) = E_0(\text{GeV})\pi/3.24$. Thus, an energy shift of 1.62 GeV from a maximum causes a $\pi/2$ rotation to a transverse polarization which produces an asymmetry consistent with zero as expected. The precession of the spin

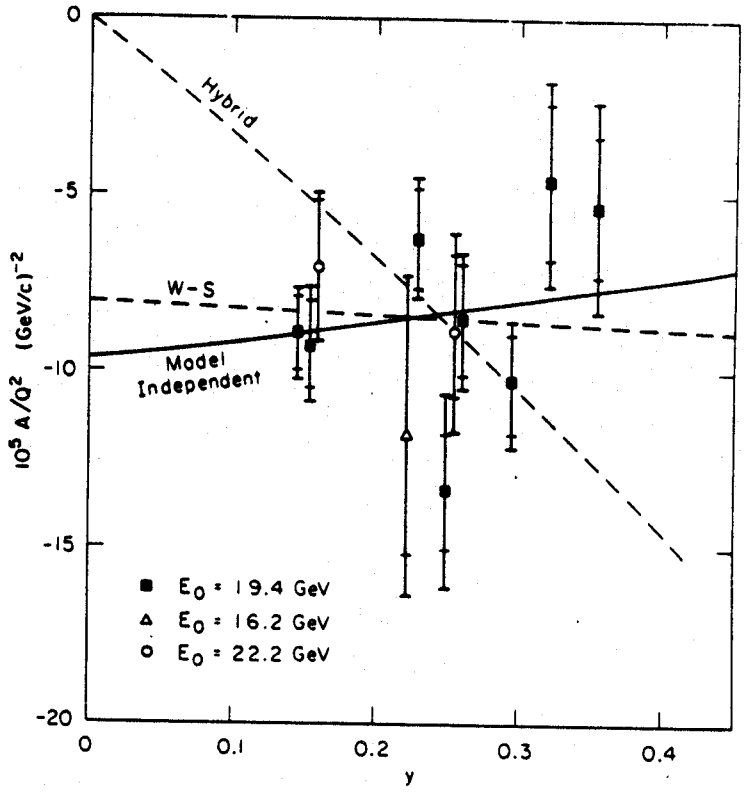

Fig. 14. The measured asymmetries for three different energies of the incident spin polarized electron beam are shown as a function of fractional energy loss $y = (E_0 - E')/E_0$. The total error bar is the combined statistical and systematic error, while the inner bar is the statistical error only. The Weinberg–Salam (W–S) model is supported by the data, but the hybrid model is ruled out. (From Prescott et al. 1979.)

polarization also provided another test, besides the prism rotation illustrated in fig. 12, of the reversal of the helicity independent of the Pockels cell.

The polarized electron scattering asymmetry is shown as a function of relative energy loss y in fig. 14. The total error bars include both statistical and systematic errors; the inner error bars are the statistical part alone. The best fits of the Weinberg–Salam (Weinberg 1967, Salam 1968) and hybrid gauge theory model predictions are also shown. The model independent line derives from fitting the results by eq. (12) with a_1 and a_2 as parameters. The authors conclude that the Weinberg–Salam model is consistent with the results within experimental errors and that the hybrid model is ruled out. A value of the Weinberg–Salam mixing parameter $\sin^2\theta_W = 0.224 \pm 0.020$ is derived from the results.

Thus, optical orientation in solids, in this case in GaAs to produce spin polarized electrons, has played a crucial role in experiments which found evidence for parity non-conservation in a neutral current interaction.

References

Alguard, M.J., W.W. Ash, G. Baum, J.G. Clendenin, P.S. Cooper, D.H. Coward, R.D. Ehrlich, A. Etkin, V.W. Hughes, H. Kobayakawa, K. Kondo, M.S. Lubell, R.H. Miller, D.A. Palmer, W. Raith, N. Sasao, K.P. Schüler, D.J. Sherden, C.K. Sinclair and P.A. Souder, 1976, Phys. Rev. Lett. **37**, 1261.

Alguard, M.J., V.W. Hughes, M.S. Lubell and P.F. Wainwright, 1977, Phys. Rev. Lett. **39**, 334.

Alvarado, S.F., F. Ciccacci, S. Valeri, M. Campagna, R. Feder and H. Pleyer, 1981a, Z. Phys. **B44**, 259.

Alvarado, S.F., F. Ciccacci and M. Campagna, 1981b, Appl. Phys. Lett. **39**, 615.

Alvarado, S., M. Campagna and H. Hopster, 1982a, Phys. Rev. Lett. **48**, 51.

Alvarado, S.F., M. Campagna, F. Ciccacci and H. Hopster, 1982b, J. Appl. Phys. **53**, 7920.

Atwood, W.B., R.L.A. Cottrell, H. DeStaebler, R. Miller, H. Pessard, C.Y. Prescott, L.S. Rochester, R.E. Taylor, M.J. Alguard, J. Clendenin, R.S. Cooper, R.D. Ehrlich, V.W. Hughes, M.S. Lubell, G. Baum, K.P. Schüler and K. Lübelsmeyer, 1978, Phys. Rev. **D18**, 2223.

Baum, B., E. Kisker, W. Raith, W. Schröder, U. Stillman and D. Zenses, 1981, J. Phys. **B14**, L97.

Bederson, B., 1969, Comm. Atom. Mol. Phys. **1**, 65.

Bederson, B., 1971, Comm. Atom. Mol. Phys. **2**, 160.

Bell, R.L., 1973, Negative Electron Affinity Devices (Clarendon Press, Oxford).

Berkovits, V.L., V.I. Safarov and A.N. Titkov, 1976, Bull. Acad. Sci. USSR, Phys. Ser. (USA) **40**, 48.

Bincer, A.M., 1957, Phys. Rev. **107**, 1434.

Burke, P.G., and J.F.B. Mitchell, 1974, J. Phys. **B7**, 214.

Bushnin, Y.B., S.V. Golovkin, R.I. Dzhelyadin, A. Zalo, A.F. Dunaitsev, A.M. Zaitsev, V.F. Konstantinov, V.P. Kubarovskii, L.G. Landsberg, V.M. Leont'ev, G.P. Makarov, V.A. Mukhin, V.G. Rybakov, T.I. Petrunina, Y.N. Simonov and V.V. Smirnov, 1976, Sov. J. Nucl. Phys. **24**, 279.

Celotta, R.J., and D.T. Pierce, 1980, Adv. Atom. Mol. Phys. **16**, 101.

Celotta, R.J., and D.T. Pierce, 1982, in: The Physics of Ionized Gases, ed. G. Pichler (Inst. of Physics of the University of Zagreb, Yugoslavia) p.3.

Ciccacci, F., S.F. Alvarado and S. Valeri, 1982, J. Appl. Phys. **53**, 4395.

Conrath, C., T. Heindorff, A. Hermanni, N. Ludwig and E. Reichert, 1979, Appl. Phys. **20**, 155.
Cooper, P.S., M.J. Alguard, R.D. Ehrlich, V.W. Hughes, H. Kobayakawa, J.S. Ladish, M.S. Lubell, N. Sasao, K.P. Schüler, P.A. Souder, G. Baum, W. Raith, K. Kondo, D.H. Coward, R.H. Miller, C.Y. Prescott, D.J. Sherden and C.K. Sinclair, 1975, Phys. Rev. Lett. **34**, 1589.
Denninger, G., V. Dose and H. Scheidt, 1979, Appl. Phys. **18**, 375.
Dingle, R., A.C. Gossard and W. Wiegmann, 1975, Phys. Rev. Lett. **34**, 1327.
Dose, V., 1977, Appl. Phys. **14**, 117.
D'yakonov, M.I., and V.I. Perel', 1974, Sov. Phys. Semicond. **7**, 1551.
Eminyan, M., and G. Lampel, 1980, Phys. Rev. Lett. **45**, 1171.
Fauster, Th., F.J. Himpsel, J.J. Donelon and A. Marx, 1983, Rev. Sci. Instrum. **54**, 68.
Feder, R., 1981, J. Phys. **C14**, 2049.
Feder, R., and H. Pleyer, 1982, Surf. Sci. **117**, 285.
Feinberg, G., 1975, Phys. Rev. **D12**, 3575.
Ford, G.W., and C.J. Mullin, 1957, Phys. Rev. **108**, 477.
Garwin, E., D.T. Pierce and H.C. Siegmann, 1974, Helv. Phys. Acta **47**, 393.
Goudsmit, S.A., and G.E. Uhlenbeck, 1925, Naturwissenschaften **13**, 1953.
Hertel, I.V., and W. Stoll, 1977, Adv. Atom. Mol. Phys. **13**, 113.
Hils, D., W. Jitschin and H. Kleinpoppen, 1982, J. Phys. **B15**, 3347.
Hughes, V.W., 1981, Internal Spin Structure of the Proton from High Energy Polarized e–p Scattering, in: High-Energy Physics with Polarized Beams and Polarized Targets, eds. C. Joseph and J. Soffer (Birkhäuser Verlag, Basel) p. 331.
Jennings, P.J., and R.O. Jones, 1982, Sol. St. Commun. **44**, 17.
Jones, R.O., and P.J. Jennings, 1983, Phys. Rev. **B21**, 4702.
Kaufmann, U., and J. Schneider, 1974, Ternary Semiconductors of Type I_B–III–VI_2 and II_B–IV–V_2, in: Festkörperprobleme Vol. 14, ed. H.J. Queisser (Pergamon Press, Oxford) p. 229.
Kessler, J., 1976, Polarized Electrons (Springer, Berlin).
Khalid, S.M., and H. Kleinpoppen, 1983, Phys. Rev. **A27**, 236.
Kisker, E., W. Gudat, E. Kuhlmann, R. Clauberg and M. Campagna, 1980, Phys. Rev. Lett. **45**, 2053.
Lampel, G., and Eminyan, 1980, J. Phys. Soc. Japan **49**, Suppl. A, 627.
Lampel, G., and C. Weisbuch, 1975, Solid State Commun. **16**, 877.
Lee, T.D., and C.N. Yang, 1956, Phys. Rev. **104**, 254.
Lubell, M.S., 1980, Polarized-Beams Studies of Spin Exchange in Electron–Hydrogen Collisions, in: Coherence and Correlation in Atomic Collisions, eds. H. Kleinpoppen and J.F. Williams (Plenum, New York) p. 663.
Lubkin, G.B., 1978, Physics Today, Sept., p. 17.
Matthews, J.W., and A.E. Blakeslee, 1976, J. Crystal Growth **32**, 265.
McDonald, A.B., 1980, in: Polarization Phenomena in Nuclear Physics, eds. C.G. Olsen, R.E. Brown, N. Jarmie, W.W. McNaughton and G.M. Hale, AIP Conf. Proc. **69**, 1358.
McDonald, A.B., 1982, private communication.
McRae, E.G., D.T. Pierce, G.-C. Wang and R.J. Celotta, 1981, Phys. Rev. **B24**, 4230.
Miller, R.C., D.A. Kleinman and A.C. Gossard, 1979, Inst. Phys. Conf. Ser. **43**, 1043.
Mills, D.L., and A.A. Maradudin, 1967, J. Phys. Chem. Solids **28**, 1855.
Mott, N.F., 1929, Proc. Roy. Soc. (London), Ser. A **124**, 425.
Osbourn, G.C., R.M. Bielfeld and P.L. Gourley, 1982, Appl. Phys. Lett. **41**, 172.
Pierce, D.T., and R.J. Celotta, 1981, Adv. Electron. Electron. Phys. **56**, 219.
Pierce, D.T., and F. Meier, 1976, Phys. Rev. **B13**, 5484.
Pierce, D.T., F. Meier and P. Zürcher, 1975a, Appl. Phys. Lett. **26**, 670.
Pierce, D.T., F. Meier and P. Zürcher, 1975b, Phys. Lett. **51A**, 465.
Pierce, D.T., R.J. Celotta, G.-C. Wang, W.N. Unertl, A. Galejs, C.E. Kuyatt and S.R. Mielczarek, 1980, Rev. Sci. Instrum. **51**, 478.

Pierce, D.T., R.J. Celotta, G.-C. Wang and E.G. McRae, 1981, Solid State Commun. **39**, 1053.
Pierce, D.T., R.J. Celotta, J. Unguris and H.C. Siegmann, 1982, Phys. Rev. B **26**, 2566.
Pollak, F.H., and M. Cardona, 1968, Phys. Rev. **172**, 816.
Prescott, C.Y., 1981, Polarized e^-e^+ Physics in Linear Colliders, in: High-Energy Physics with Polarized Beams and Polarized Targets, eds. C. Joseph and J. Soffer (Birkhäuser Verlag, Basel) p. 34.
Prescott, C.Y., W.B. Atwood, R.L.A. Cottrell, H. De Staebler, E.L. Garwin, A. Gonidec, R.H. Miller, L.S. Rochester, T. Sato, D.J. Sherden, C.K. Sinclair, S. Stein, R.E. Taylor, J.E. Clendenin, V.W. Hughes, N. Sasao, K.P. Schüler, M.G. Borghini, K. Lübelsmeyer and W. Jentschke, 1978, Phys. Lett. **77B**, 347.
Prescott, C.Y., W.B. Atwood, R.L.A. Cottrell, H. De Staebler, E.L. Garwin, A. Gonidec, R.H. Miller, L.S. Rochester, T. Sato, D.J. Sherden, C.K. Sinclair, S. Stein, R.E. Taylor, C. Young, J.E. Clendenin, V.W. Hughes, N. Sasao, K.P, Schüler, M.G. Borghini, L. Lübelsmeyer and W. Jentschke, 1979, Phys. Lett. **84B**, 524.
Rado, G.T., 1957, Bull. Am. Phys. Soc. II, **2**, 127.
Ravano, G., M. Erbudak and H.C. Siegmann, 1982, Phys. Rev. Lett. **49**, 80.
Reichert, E., and K. Zähringer, 1982, Appl. Phys. **A29**, 191.
Reihl, B., M. Erbudak and D.M. Campbell, 1979, Phys. Rev. **B19**, 6358.
Salam, A., 1968, in: Elementary particle theory: relativistic groups and analyticity, Nobel Symp. No. 8, ed. N. Svartholm (Almqvist and Wiksel, Stockholm) p. 367.
Shay, J.L., and J.H. Wernick, 1975, Ternary Chalcopyrite Semiconductors: Growth, Electronic Properties and Applications (Pergamon Press, Oxford) p. 79.
Shull, C.G., C.T. Chase and F.E. Myers, 1943, Phys. Rev. **63**, 29.
Siegmann, H.C., D.T. Pierce and R.J. Celotta, 1981, Phys. Rev. Lett. **46**, 452.
Siegmann, H.C., F. Meier, M. Erbudak and M. Landolt, 1984, Adv. Electron. Electron. Phys., vol. 62.
Sinclair, C.K., 1981, High Intensity Polarized Electron Sources, in: High-Energy Physics with Polarized Beams and Polarized Targets, eds. C. Joseph and J. Soffer (Birkhäuser Verlag, Basel).
Sinclair, C.K., and R.H. Miller, 1981, IEEE Trans. Nucl. Sci. NS **28**, 2649.
Sinclair, C.K., E.L. Garwin, R.H. Miller and C.Y. Prescott, 1976, in: High-Energy Physics with Polarized Beams and Targets, AIP Conf. Proc. **35**, 424.
Spicer, W.E., 1958, Phys. Rev. **112**, 114.
Unguris, J., A. Seiler, R.J. Celotta, D.T. Pierce, P.D. Johnson and N.V. Smith, 1982, Phys. Rev. Lett. **49**, 1047.
Unguris, J., D.T. Pierce and R.J. Celotta, 1984, Phys. Rev. **B29**, 1381.
Weinberg, S., 1967, Phys. Rev. Lett. **19**, 1264.
Woodruff, D.P., and N.V. Smith, 1982, Phys. Rev. Lett. **48**, 283.
Wübker, W., R. Mollenkamp and J. Kessler, 1982, Phys. Rev. Lett. **49**, 272.
Zorabedian, P., 1982, SLAC Report 248.
Zürcher, P., and F. Meier, 1979, J. Appl. Phys. **50**, 3687.